

Near-infrared Laser-induced Temperature Elevation in Optically-trapped Aqueous Droplets in Air

Shoji ISHIZAKA,*† Jiang MA,* Terufumi FUJIWARA,* Kunihiro YAMAUCHI,** and Noboru KITAMURA**

*Department of Chemistry, Graduate School of Science, Hiroshima University, Kagamiyama, Higashi-hiroshima 739-8526, Japan

**Department of Chemistry, Faculty of Science and Department of Chemical Sciences and Engineering, Graduate School of Chemical Sciences and Engineering, Hokkaido University, Sapporo 060-0810, Japan

Near-infrared laser-induced temperature elevation in single aqueous ammonium sulfate droplets levitated in air were evaluated by means of laser trapping and Raman spectroscopy. Since the vapor pressure in an aqueous solution droplet should be thermodynamically in equilibrium with that of water in air, the equilibrium size of the droplet varies sensitively through evaporation/condensation of water in accordance with the temperature change of the droplet. In this study, we demonstrated that the changes in the size of an optically levitated aqueous ammonium sulfate droplet were induced by irradiation of a 1064-nm laser beam as a heat source under an optical microscope. Temperature elevation in the droplet was evaluated successfully by means of Raman spectroscopy, and the values determined were shown to be in good agreement with those by the theoretical calculations based on the absorption coefficient of water at 1064-nm and the thermal conductivity of air. To the best of our knowledge, this is the first experimental demonstration showing that the absorption coefficient evaluated from changes in the size of optically-trapped aqueous droplets is consistent with that of pure water.

Keywords Laser trapping, Raman spectroscopy, aerosol

(Received October 12, 2015; Accepted November 24, 2015; Published April 10, 2016)

Introduction

A focused near-infrared (NIR) laser beam has a high potential for both inducing thermally-induced phenomena and manipulation of various materials under an optical microscope.¹⁻⁵ As an example, we previously reported that thermal phase separation of an aqueous triethylamine (TEA) solution was induced by the laser beam irradiated under an optical microscope, and a single micrometer-sized TEA droplet generated in the solution phase was trapped simultaneously by the incident laser beam.⁴ Since water (H₂O) absorbs incident 1064-nm laser light through the overtone band of the OH stretching vibration mode, this results in heat generation in the vicinity of the focal spot of the laser beam and, thereby, photothermal phase separation of an aqueous TEA solution. On the basis of the phase diagram of a TEA/H₂O system, the temperature elevation induced by the 1064-nm laser beam (1.5 W) was roughly estimated to be 3–5 K. A quantitative measurement of the temperature at the focal point of laser light under an optical microscope is an indispensable basis for interpretation of such thermally-induced phenomena in a micrometer dimension. Experimental studies on local heating in the focus of an optical trap have been hitherto reported for various systems.⁶⁻¹⁸ However, the number of the reports on estimation of the amount of heat generation through absorption of a photon energy by single optically-trapped water

droplets in air is still limited.¹⁴⁻¹⁸ In order to achieve the quantitative measurement of temperature elevation of optically-trapped water droplets in air, we employed a 1064-nm laser beam as a heating light source.

Noncontact levitation of a single micrometer-sized water droplet in air can be achieved by a laser trapping technique.¹⁹⁻²⁸ Furthermore, a laser beam used as a trapping light source can be used simultaneously as an excitation light source for Raman spectroscopy, which provides an opportunity to study a droplet size in nanometer accuracy. The equilibrium size of a trapped water droplet in air varies sensitively through water evaporation/condensation in accordance with relative humidity (RH), temperature, and solute concentration. On the basis of such characteristic features of an aerosol water droplet, Reid *et al.* have reported heat generation in an optically-trapped aqueous sodium chloride droplet upon 532-nm laser beam irradiation.¹⁶⁻¹⁸ In practice, it was demonstrated that the modulation in the laser power of the 532-nm light beam of a few mW gave rise to a modulation in the droplet temperature of a few mK and size changes on the order of 1 nm in radius. Although the experimental approach is quite unique and useful for high-sensitive absorption measurements of individual aerosol water droplets, the absorption coefficients determined by the experiments (1.03×10^{-1} – 1.51×10^{-1} m⁻¹) are larger than that of pure water (4.3×10^{-2} m⁻¹ at 532 nm). They concluded that the discrepancy between the experiments and theoretical prediction was attributed to absorption of trace amounts of impurities contaminated in sodium chloride. Since the absorption coefficient of water at 532 nm is extremely low,

† To whom correspondence should be addressed.
E-mail: ishizaka@hiroshima-u.ac.jp

temperature elevation arising from the impurities would not be ignored. For further advances in the evaluation and interpretation of local heating in an aerosol water droplet under an optical microscope, therefore, such a study is worth exploring by using an NIR laser beam as a heating light source. Water absorbs 1064-nm laser light through the overtone band of the OH stretching vibration mode as described above and the absorption coefficient of water at 1064 nm (14.5 m^{-1}) is much higher than that at 532 nm ($4.3 \times 10^{-2} \text{ m}^{-1}$). Therefore, a 1064-nm laser beam is suitable as a heating light source for evaluation of generated heat in an optically-trapped aerosol water droplet.

In the present study, we constructed a laser trapping—Raman spectroscopy system capable of determination of 1064-nm laser-induced temperature elevation in single aerosol water droplets. Using the developed system, we demonstrate that the change in the size of a trapped aqueous ammonium sulfate droplet is induced by 1064-nm laser irradiation. On the basis of the Köhler theory, furthermore, we succeeded in determining temperature elevation in the trapped aerosol water droplet as a function of 1064-nm laser power. We will also discuss the amounts of laser-induced heat generation in single water droplets in respect to the absorption coefficient of water at 1064 nm and the thermal conductivity of air.

Experimental

Laser trapping-Raman microspectroscopy system

A schematic illustration of the experimental setup used in the present study is shown in Fig. 1. An aqueous ammonium sulfate solution ($[(\text{NH}_4)_2\text{SO}_4] = 0.10 \text{ mol dm}^{-3}$) was nebulized and

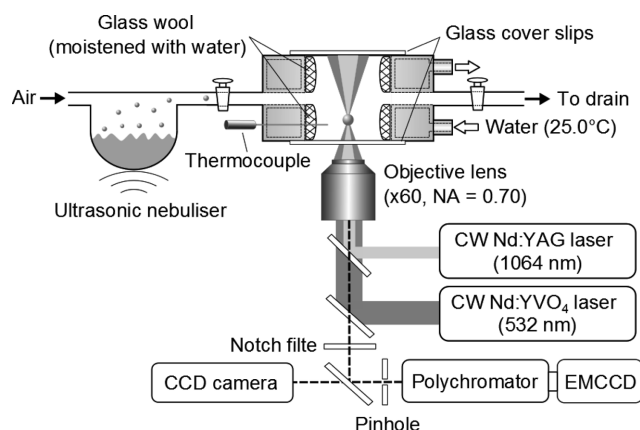


Fig. 1 Schematic illustration of laser trapping and Raman spectroscopic system.

introduced to a chamber (internal diameter of 4 cm and a height of 4 cm) set on the stage of an inverted optical microscope (Olympus, IX71). In order to keep the relative humidity within the chamber constant, the inner wall of the chamber was covered with a glass wool moistened with pure water. The temperature inside the chamber was kept constant at $298.05 \pm 0.01 \text{ K}$ by flowing thermostat water (Yamato Scientific Co., Ltd., Thermo-Elite BH51) to the outer jacket of the chamber (see also Fig. 1), and was monitored by a thermocouple (IWATU, SC-0107) set inside the chamber. Single micrometer-sized water droplets were trapped by a focused 532-nm laser beam from a CW-Nd:YVO₄ laser (Coherent, Verdi V2) through a dry objective (Olympus LUCPLFLN 60 \times , N.A. = 0.70) equipped with a correction collar. The 532-nm laser beam was simultaneously used as an excitation light source for Raman spectroscopy. A 1064-nm laser beam from a CW-Nd:YAG laser (Laser-Export Co. Ltd., LCS-DTL-322-1000) was introduced coaxially with the 532-nm laser beam into the chamber as a heating light source. Laser power of the 1064-nm light beam passed through the objective lens and a glass cover slip (P_{1064}) was measured by a photodiode sensor (Ophir Optonics Solutions Ltd., PD300-SH). Raman spectra of the trapped droplet with or without 1064-nm laser irradiation were measured by using a cooled EMCCD detector (ANDOR, Newton DU970N-BV) equipped with a polychromator (SOLAR TII, MS3504i, 300 or 1200 grooves/mm). Bright-field images under the microscope were observed by using a CCD camera (TOSHIBA TELI, CS9301-03).

Chemicals

Water was purified by reverse osmosis and deionization prior to use (Merck Millipore, Milli-Q Integral 3). Ammonium sulfate (Wako Pure Chemical Co., Ltd.) was used without further purification.

Results and Discussion

In situ quantification of ammonium sulfate in single water droplets by means of laser trapping and Raman spectroscopy

Single micrometer-sized aqueous ammonium sulfate droplets in air were trapped successfully by focused 532-nm laser beam irradiation. A typical example of the photograph of a single trapped droplet is shown in Fig. 2A. After trapping, the flow of the water droplets from the nebulizer was stopped and, the inlet/outlet valves of the chamber were closed. After all of the non-trapped water droplets fell down onto the bottom glass coverslip, the trapped droplet was kept in the chamber more than 30 min until the droplet began to reach a thermodynamic equilibrium. The equilibrium size of the trapped water droplet depends on both $[(\text{NH}_4)_2\text{SO}_4]$ and temperature in the droplet. For discussion

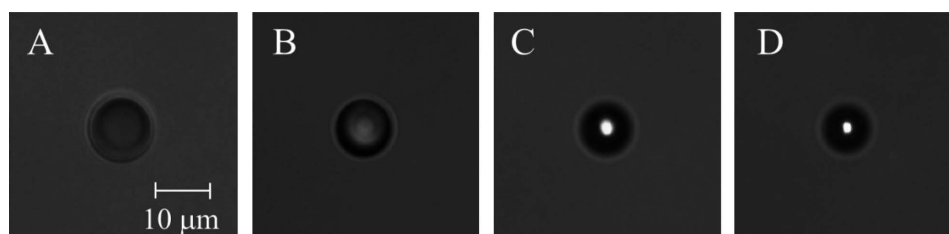


Fig. 2 Optical micrographs of a single aqueous ammonium sulfate droplet levitated in air in the absence (A) or presence of 1064-nm laser irradiation at $P_{1064} = 0.99$ (B), 1.98 (C), and 3.12 mW (D).

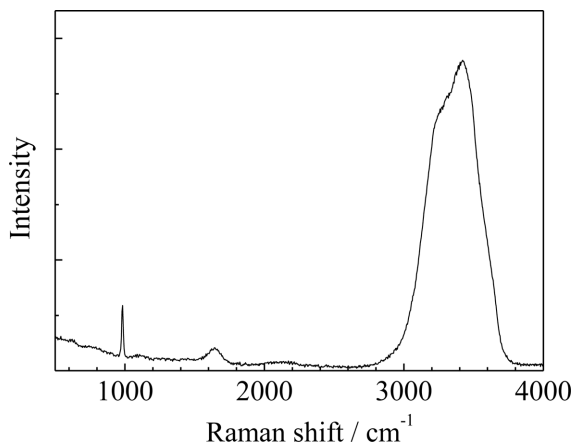


Fig. 3 Raman spectrum of the aqueous ammonium sulfate droplet (Fig. 2A) in the absence of 1064-nm laser irradiation.

on temperature elevation in the droplet, one must know $[(\text{NH}_4)_2\text{SO}_4]$ in the droplet, since the concentration in the droplet is not necessarily equal to that of the mother solution as reported previously.¹⁹ Therefore, we determined $[(\text{NH}_4)_2\text{SO}_4]$ in the droplet by *in situ* Raman microspectroscopy. The Raman spectrum observed by monitoring that from the central region of the droplet (Fig. 2A) is shown in Fig. 3. The peaks observed at 980 and 3420 cm^{-1} are assigned to the symmetric stretching vibration of a SO_4^{2-} anion and the OH stretching vibrations of water, respectively. As reported in the previous publications, the ratio of the Raman intensity of the 980 cm^{-1} band to that of the 3420 cm^{-1} band, I_{980}/I_{3420} , is linearly proportional to $[(\text{NH}_4)_2\text{SO}_4]$ in water.²⁰ On the basis of the observed Raman intensity ratio ($I_{980}/I_{3420} = 0.210$) in Fig. 3 and the relationship between I_{980}/I_{3420} and $[(\text{NH}_4)_2\text{SO}_4]$ reported previously,²⁰ the $(\text{NH}_4)_2\text{SO}_4$ concentration in the droplet was determined to be 0.147 mol dm^{-3} , which was higher than that of the mother solution ($[(\text{NH}_4)_2\text{SO}_4] = 0.100 \text{ mol dm}^{-3}$).

Raman scattering observed by monitoring that from the peripheral region of the droplet can be used to determine the droplet radius in nanometer accuracy.²⁸ The Raman spectrum of the droplet in the OH stretching vibration region thus observed is shown in Fig. 4A. It is worth noting that several sharp peaks are superimposed to the broad OH stretching vibration band. Since the refractive index of water (1.33) is higher than that of air (1.00), Raman scattering light from the inside of the droplet is reflected totally at the droplet/air boundary and propagates circumferentially to produce the standing waves at the boundary. This phenomenon is called whispering gallery mode (WGM) resonances, which coincides with the cavity resonance wavelengths.^{20,27–29} The WGM resonances can be analyzed on the basis of Mie scattering theory.³⁰ The scattering efficiency (Q_s) of a microsphere is given by Eq. (1).

$$Q_s = \frac{2}{x^2} \sum_{n=1}^{\infty} (2n+1) (|a_{n,l}|^2 + |b_{n,l}|^2) \quad (1)$$

$x = 2\pi r/\lambda$ is known as the size parameter, and r and λ are the radius of the microsphere and the wavelength of scattered light, respectively. The coefficients $a_{n,l}$ and $b_{n,l}$ are the spherical Bessel and Hankel functions of the first kind, respectively.

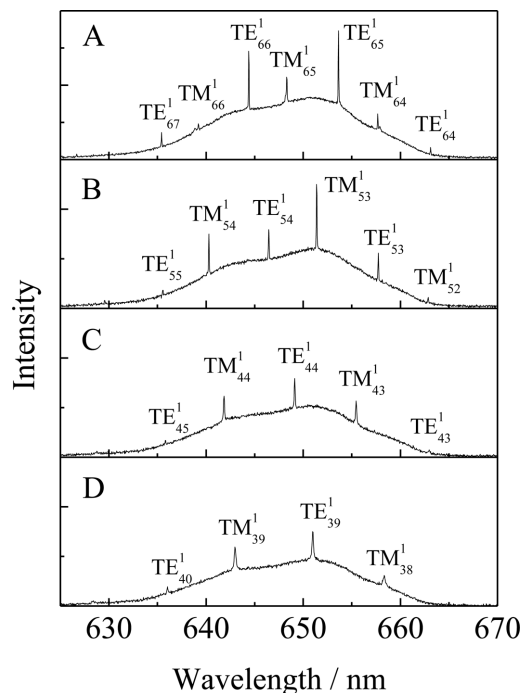


Fig. 4 The Raman scattering from the peripheral region of the droplet in the absence (A) or presence of 1064-nm laser beam irradiation at $P_{1064} = 0.99$ (B), 1.98 (C), and 3.12 mW (D).

$$a_{n,l} = \frac{j_n(x)[mxj_n(mx)] - m^2 j_n(mx)[xj_n(x)]}{h_n^{(0)}(x)[mxj_n(mx)] - m^2 j_n(mx)[xh_n^{(0)}(x)]} \quad (2)$$

$$b_{n,l} = \frac{j_n(x)[mxj_n(mx)] - j_n(mx)[xj_n(x)]}{h_n^{(0)}(x)[mxj_n(mx)] - j_n(mx)[xh_n^{(0)}(x)]} \quad (3)$$

The integer n denotes the order of the spherical Bessel and Hankel functions known as the angular mode number and l represents the mode order of the resonance. In Eqs. (2) and (3), m represents the real part of the refractive index of water, which depends on the solute concentration in the droplet. In the present study, we took into account dependence of the m values on $[(\text{NH}_4)_2\text{SO}_4]$.³¹ On the basis of $[(\text{NH}_4)_2\text{SO}_4]$ determined by the Raman intensity ratio (I_{980}/I_{3420}), the m value of the droplet (Fig. 2A) is estimated to be 1.336. The wavelengths of the WGMs in Fig. 4A can be used to calculate the droplet size by an iterative simulation of the resonant fingerprints based on Eq. (1).^{20,27,28} The assignment of each resonant mode is included in Fig. 4A. The transverse electric and transverse magnetic modes are abbreviated by TE and TM, respectively, and the superscript and subscript denote the mode order and number, respectively, in Fig. 4A. The radius of the droplet (Fig. 2A) without 1064-nm laser irradiation is then determined to be 5.577 μm . Knowing the size of the droplet, one can evaluate the amount of $(\text{NH}_4)_2\text{SO}_4$ (N) solubilized in the droplet to be $1.07 \times 10^{-13} \text{ mol}$. Since $(\text{NH}_4)_2\text{SO}_4$ is nonvolatile, the N value should be constant irrespective of the size of a water droplet.²⁸ In order to evaluate the amount of temperature elevation in the droplet upon 1064-nm laser beam irradiation, we employ the N value determined by Raman spectroscopy in the following analysis.

Table 1 The equilibrium size change and temperature elevation of the optically-trapped droplet induced by near-infrared laser irradiation

P_{1064}/mW	$r/\mu\text{m}$	$\Delta T_{532}/\text{K}^a$	$\Delta T_{1064}/\text{K}^a$	$\Delta T_{\text{size}}/\text{K}^b$
A 0	5.577	5.3×10^{-3}	0	0
B 0.99	4.577 ± 0.269	5.3×10^{-3}	0.09	0.08 ± 0.03
C 1.98	3.802 ± 0.096	5.3×10^{-3}	0.18	0.19 ± 0.03
D 3.12	3.444 ± 0.077	5.3×10^{-3}	0.28	0.28 ± 0.02

a. ΔT_{532} and ΔT_{1064} values were calculated from Eq. (7) on the basis of the Beer-Lambert law.

b. ΔT_{size} values were calculated on the basis of the Köhler theory.

The near-infrared laser power dependence of the equilibrium size of a water droplet in air

The photographs of the trapped droplet under 1064-nm laser irradiation are shown in Figs. 2B – 2D. While the power of the 532-nm laser beam was constant at 20 mW, that of the 1064-nm laser beam was controlled from $P_{1064} = 0.99 - 3.12$ mW. As seen in Fig. 2, the equilibrium size of the droplet decreased with increasing P_{1064} . To assess the experimental errors, Raman spectra of the droplet were measured at least four times at each P_{1064} conditions. The typical Raman spectra of the droplets relevant to Figs. 2B – 2D are shown in Figs. 4B – 4D. The radius of each water droplet shown in Figs. 2B – 2D was determined by the Mie scattering calculations as explained above. The averaged radii at each P_{1064} conditions are summarized in Table 1.

In order to estimate the flux of energy absorbed by the droplet, one must consider the profile of the beam interacting with the droplet. In the experiments of optical trapping of aqueous droplets in air, an aqueous layer is often deposited on a coverslip, which arises as a result of non-trapped water droplets from a nebulizer. Therefore, the laser beam is focused through several media of different refractive indices, glass coverslip ($m = 1.52$), aqueous layer ($m = 1.33$) and air ($m = 1.00$), before reaching the trapped droplet. When using high numerical aperture objectives, minute variations in cover glass thickness and dispersion properties become a source of spherical aberration and lead to broadening of the beam waist at the focal point. Miles *et al.* have pointed out that the beam waist at a trapping site must be considered to estimate the absorption efficiency of single optically-trapped aqueous droplets, and indicated that the magnitude of the resonant absorption efficiency increase with increasing the size of beam waist on the basis of generalized Lorenz-Mie theory.¹⁸ On the other hand, in order to compensate for the mismatches in the refractive indices, a dry objective equipped with a correction collar was employed in this study. Therefore, the contribution from resonant absorption to the temperature elevation in the droplet will be negligibly small in the present experiments. Furthermore, since absorption of single particles as small as $r = 4 \mu\text{m}$ has been successfully analyzed by the simple Beer-Lambert law as demonstrated in the previous papers,^{32,33} the Beer-Lambert law was employed in the following calculation.

In a steady state, it can be assumed that the generated heat (Q) in a water droplet by optical absorption of incident 1064- or 532-nm light should be in balance with cooling by heat conduction from the droplet to the surrounding medium (*i.e.*, humid air). If this is the case, temperature elevation of the droplet can be calculated theoretically based on light power ($P = P_{1064}$ or P_{532}), the α of water at 1064- or 532-nm, and the thermal conductivity of humid air. On the basis of the Beer-

Lambert law, the Q value can be estimated by Eq. (4),

$$Q = [1 - \exp(-2r\alpha)] \times P \quad (4)$$

where $2r$ is the diameter of the droplet as an optical path length for photoabsorption. The α values at 532 and 1064 nm are 4.3×10^{-2} and 14.5 m^{-1} , respectively.^{10,16} When local heat is equilibrated by the surrounding gas phase, the temperature elevation (ΔT) of the droplet can be calculated by Eq. (5),

$$\Delta T_{532/1064} = \frac{Q}{4\pi r \kappa} \quad (5)$$

where κ is the thermal conductivity of humid air ($25.77 \times 10^{-3} \text{ W m}^{-1} \text{ K}^{-1}$) at 25.0°C .³⁴ In the case of a micrometer-sized water droplet, since the $(-2r\alpha)$ value in Eq. (4) is extremely small ($\ll 1$), Eqs. (4) and (5) can be approximated by Eqs. (6) and (7), respectively.

$$Q = [1 - \exp(-2r\alpha)] \times P \approx 2r\alpha P. \quad (6)$$

$$\Delta T_{532/1064} = \frac{Q}{4\pi r \kappa} \approx \frac{\alpha}{2\pi \kappa} P. \quad (7)$$

Equation (7) predicts that the amount of local heat in the droplet increases in proportion to P and is independent of the droplet size. The temperature elevation in the droplet induced by 532- (ΔT_{532}) and 1064-nm laser irradiation (ΔT_{1064}) calculated are summarized in Table 1. In the present experiments, P_{532} is kept constant at 20 mW, the ΔT_{532} value is constant at $5.3 \times 10^{-3} \text{ K}$ irrespective of the change in the optical path length. On the other hand, the ΔT_{1064} value increases with increasing P_{1064} as seen in Table 1. The results clearly suggest that heat generated by absorption of 1064-nm laser light is the main factor that governs the change in the size of the trapped water droplet (Figs. 2B – 2D).

Evaluation of the temperature elevation of the droplet on the basis of the Köhler theory

Since the vapor pressure of water at the droplet surface should be equal to the partial pressure of water in air, the temperature elevation of the droplet can be also evaluated by calculating the vapor pressure of the trapped water droplet with or without 1064-nm laser irradiation. The equilibrium vapor pressure of a droplet containing a highly soluble substance such as $(\text{NH}_4)_2\text{SO}_4$, NaCl, or H_2SO_4 can be described by the Köhler theory,^{35,36} and the simplest form by the theory for an aqueous solution droplet is given by Eq. (8),

$$S = \frac{e_s(r)}{e_s(\infty)} \approx 1 + \frac{a}{r} - \frac{b}{r^3} \quad (8)$$

where S is the ratio of the vapor pressure of water over a droplet surface containing a solute ($e_s(r)$) to that over a flat surface without a solute ($e_s(\infty)$), a and b represent the influence of surface tension of a droplet (the Kelvin effect) and the vapor pressure reduction by a dissolved solute (the Raoult's law), respectively.

$$a = \frac{2\sigma m_v}{\rho_w R_s T} \quad (9)$$

$$b = \frac{3im_v M}{4\pi \rho_w m_s} \quad (10)$$

In Eqs. (9) and (10), σ is the surface tension of a water droplet, ρ_w is the density of a solution and, m_v and m_s are the molecular weights of water (18.016 g mol⁻¹) and a solute (*i.e.*, ammonium sulfate, 132.14 g mol⁻¹), respectively. R_v and T represent the gas constant for water vapor ($R_v = 461 \text{ J K}^{-1} \text{ kg}^{-1}$) and the absolute temperature (298.05 K), respectively. M is the mass of a solute and i is the van't Hoff factor. As discussed in the previous section, the amount of ammonium sulfate ($N = M/m_s$) in the trapped droplet is constant at $1.07 \times 10^{-13} \text{ mol}$. In the calculations of a and b , we must consider the influence of the solute concentration on σ and i . Thus, both σ and i values were determined by extrapolation from the literature values.^{37,38} According to the Magnus-Tetens approximation, the vapor pressure of water over a flat surface at a given temperature is calculated by Eq. (11).³⁹

$$e_s(\infty) = 610.78 \exp \left[17.2693882 \frac{(T - 273.16)}{(T - 35.86)} \right]. \quad (11)$$

At 298.05 K, the $e_s(\infty)$ value is 3147 Pa and S without 1064-nm laser irradiation can be calculated to be 0.9942 on the basis of Eq. (8). Thus, the vapor pressure of water at the droplet surface (Fig. 2A) is calculated to be $e_s(r) = S \times e_s(\infty) = 3129 \text{ Pa}$. These results indicate that the partial pressure of water in the surrounding gas phase is 3129 Pa, corresponding to RH of 99.42%.

Upon 1064-nm laser irradiation to the droplet, an increase in temperature causes that in $e_s(r)$. This leads to evaporation of the droplet, while evaporation of the droplet results in a decrease in the droplet size and an increase in the solute concentration, giving rise to lowering in $e_s(r)$ (Raoult's law). When the droplet size decreases, the vapor pressure of the droplet ($e_s(r)$) varies to attain an equilibrium with that of surrounding air (3129 Pa), giving a new equilibrium droplet size at a given temperature. Since the volume of the chamber is much larger than that of the trapped water droplet, the RH of air in the chamber would not be affected by evaporation of a small amount of water from the droplet as in the present experiment. Consequently, the $e_s(r)$ value should be constant at 3129 Pa with and without 1064-nm laser irradiation. Since the temperature dependence of the vapor pressure of a water droplet would be evaluated by the Magnus-Tetens approximation (Eq. (11)), the amount of a temperature jump upon laser irradiation (ΔT_{size}) was calculated by the changes in the size of the droplet. On the basis of Eqs. (8) – (11), the ΔT_{size} value under given 1064-nm laser power (B – D) calculated is included in Table 1. As seen in Table 1, it is worth emphasizing that the ΔT_{size} values are in good agreement with the ΔT_{1064} values calculated on the basis of the Beer-Lambert law. As predicted by Eq. (7), furthermore, the ΔT_{size} value showed a linear relationship with incident 1064-nm laser power (P_{1064}) as shown in Fig. 5. A least-means squares fitting of the data in Fig. 5 demonstrated the slope value to be 90.8 K/W. On the basis of the slope value and Eq. (7), we obtained the α to be 14.7 m^{-1} , which agreed very well with the literature values: $14.2 - 14.5 \text{ m}^{-1}$ at 1064 nm.^{6,10,40,41} This clearly indicates that the temperature elevation in the droplet can be ascribed to absorption of the 1064-nm laser beam by water molecules. To the best of our knowledge, this is the first experimental demonstration showing that the absorption coefficient evaluated from changes in the size of optically-trapped aqueous droplets is consistent with that of pure water.

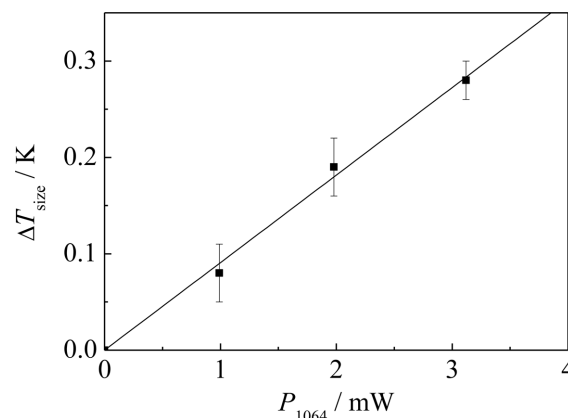


Fig. 5 The relationship between ΔT_{size} and the 1064-nm laser power (P_{1064}). Solid line represents the least-squares fit to the observed data.

Conclusions

It is easily predicted that a micrometer-sized water droplet in air is very likely to evaporate through subtle changes in the temperature and/or vapor pressure of the droplet and, thus, this gives rise to the change in the droplet size. Although such circumstances sometimes disturbs experimental studies on single aerosol water droplets, one can evaluate directly the temperature in a single laser-trapped aerosol water droplet through the size change of the droplet. As demonstrated in the present study, in practice, temperature elevation in a single aerosol water droplet induced by 1064-nm laser irradiation was evaluated successfully by means of cavity enhanced Raman spectroscopy, and the amounts of temperature elevation determined experimentally were in good agreement with theoretical calculations on the basis of the absorption coefficient of water at 1064-nm and the thermal conductivity of air.

Micrometer-sized aerosol droplets play key roles in both fundamental and applied research fields, represented by atmospheric chemistry, chemical vapor deposition, nanoparticle synthesis, and so on. The laser trapping-microspectroscopy (absorption/emission/Raman) technique is the powerful means to manipulate and interrogate an arbitrary sized single droplet in the gas phase. Since the temperature elevation induced by laser irradiation is one of the most important information to understand the various physical and chemical responses or phenomena of single droplets levitated in air. Therefore, the present results would provide an indispensable basis for studies on aerosol chemistry by using the laser trapping technique.

Acknowledgements

This research was supported by a Grand-in-Aid for Scientific Research (C) (No. 25410144) from the Ministry of Education, Culture, Sports, Science, and Technology (MEXT), Japan.

References

1. M. Ishikawa, H. Misawa, N. Kitamura, and H. Masuhara, *Chem. Lett.*, **1993**, 22, 481.
2. M. Ishikawa, H. Misawa, N. Kitamura, R. Fujisawa, and H. Masuhara, *Bull. Chem. Soc. Jpn.*, **1996**, 69, 59.

3. S. A. Mukai, N. Magome, H. Kitahata, and K. Yoshikawa, *Appl. Phys. Lett.*, **2003**, *83*, 2557.
 4. N. Kitamura, M. Yamada, S. Ishizaka, and K. Konno, *Anal. Chem.*, **2005**, *77*, 6055.
 5. Y. Tsuboi, M. Nishino, T. Sasaki, and N. Kitamura, *J. Phys. Chem. B*, **2005**, *109*, 7033.
 6. E. J. G. Peterman, F. Gittes, and C. F. Schmidt, *Biophys. J.*, **2003**, *84*, 1308.
 7. P. M. Celliers and J. Conia, *Appl. Optics*, **2000**, *39*, 3396.
 8. Y. Liu, G. J. Sonek, M. W. Berns, and B. J. Tromberg, *Biophys. J.*, **1996**, *71*, 2158.
 9. A. Kiraz, Y. Karadag, and M. Muradoglu, *Phys. Chem. Chem. Phys.*, **2008**, *10*, 6446.
 10. S. Ito, T. Sugiyama, N. Toitani, G. Katayama, and H. Miyasaka, *J. Phys. Chem. B*, **2007**, *111*, 2365.
 11. D. F. Zhao, T. Zhu, Q. Chen, Y. J. Liu, and Z. F. Zhang, *Sci. Chin. Chem.*, **2011**, *54*, 154.
 12. S. Wurlitzer, C. Lautz, M. Liley, C. Duschl, and T. M. Fischer, *J. Phys. Chem. B*, **2001**, *105*, 182.
 13. Y. Liu, D. K. Cheng, G. J. Sonek, M. W. Berns, C. F. Chapman, and B. J. Tromberg, *Biophys. J.*, **1995**, *68*, 2137.
 14. J. Popp, M. Lankers, K. Schaschek, W. Kiefer, and J. T. Hodges, *Appl. Optics*, **1995**, *34*, 2380.
 15. M. Guillon, R. E. H. Miles, J. P. Reid, and D. McGloin, *New J. Phys.*, **2009**, *11*, 103041.
 16. K. J. Knox and J. P. Reid, *J. Phys. Chem. A*, **2008**, *112*, 10439.
 17. R. E. H. Miles, M. Guillon, L. Mitchem, D. McGloin, and J. P. Reid, *Phys. Chem. Chem. Phys.*, **2009**, *11*, 7312.
 18. R. E. H. Miles, J. S. Walker, D. R. Burnham, and J. P. Reid, *Phys. Chem. Chem. Phys.*, **2012**, *14*, 3037.
 19. S. Ishizaka, K. Yamauchi, and N. Kitamura, *Anal. Sci.*, **2013**, *29*, 1223.
 20. S. Ishizaka, K. Yamauchi, and N. Kitamura, *Bunseki Kagaku*, **2013**, *62*, 361.
 21. A. Ashkin and J. M. Dziedzic, *Science*, **1975**, *187*, 1073.
 22. N. Magome, M. I. Kohira, E. Hayata, S. Mukai, and K. Yoshikawa, *J. Phys. Chem. B*, **2003**, *107*, 3988.
 23. R. J. Hopkins, L. Mitchem, A. D. Ward, and J. P. Reid, *Phys. Chem. Chem. Phys.*, **2004**, *6*, 4924.
 24. L. Mitchem, J. Buajarern, R. J. Hopkins, A. D. Ward, R. J. Gilham, R. L. Johnston, and J. P. Reid, *J. Phys. Chem. A*, **2006**, *110*, 8116.
 25. G. Hargreaves, N. O. A. Kwamena, Y. H. Zhang, J. R. Butler, S. Rushworth, S. L. Clegg, and J. P. Reid, *J. Phys. Chem. A*, **2010**, *114*, 1806.
 26. S. Ishizaka, T. Wada, and N. Kitamura, *Chem. Phys. Lett.*, **2011**, *506*, 117.
 27. S. Ishizaka, Y. Suzuki, and N. Kitamura, *Phys. Chem. Chem. Phys.*, **2010**, *12*, 9852.
 28. S. Ishizaka, K. Yamauchi, and N. Kitamura, *Anal. Sci.*, **2014**, *30*, 1075.
 29. R. Symes, R. M. Sayer, and J. P. Reid, *Phys. Chem. Chem. Phys.*, **2004**, *6*, 474.
 30. P. W. Barber and S. C. Hill, "Light Scattering by Particles: Computational Methods", **1990**, World Scientific Publishing Co. Pte. Ltd., Singapore.
 31. Landolt-Börnstein, "Physikalische-chemische Tabellen", **1923**, Springer-Verlag.
 32. H. B. Kim, S. Yoshida, and N. Kitamura, *Anal. Chem.*, **1998**, *70*, 51.
 33. H. B. Kim, S. Yoshida, A. Miura, and N. Kitamura, *Anal. Chem.*, **1998**, *70*, 111.
 34. P. T. Tsilingiris, *Energy Convers. Manage.*, **2008**, *49*, 1098.
 35. H. Köhler, *Trans. Faraday Soc.*, **1936**, *32*, 1152.
 36. A. Laaksonen, P. Korhonen, M. Kulmala, and R. J. Charlson, *J. Atmos. Sci.*, **1998**, *55*, 853.
 37. E. R. Lewis, *J. Aerosol Sci.*, **2006**, *37*, 1605.
 38. R. D. H. Low, *J. Atmos. Sci.*, **1969**, *26*, 608.
 39. F. W. Murray, *J. Appl. Meteorol.*, **1967**, *6*, 203.
 40. G. M. Hale and M. R. Querry, *Appl. Optics*, **1973**, *12*, 555.
 41. L. H. Kou, D. Labrie, and P. Chylek, *Appl. Optics*, **1993**, *32*, 3531.
-